Ensemble firing of muscle afferents recorded during normal locomotion in cats

Arthur Prochazka and Monica Gorassini

Division of Neuroscience, University of Alberta, Edmonton, Alberta, Canada T6G 2S2

(Received 18 July 1997; accepted after revision 16 October 1997)

1. The main purpose of this study was to collate population data on the firing characteristics of muscle afferents recorded chronically during normal stepping in cats.

2. Ensemble firing profiles of forty-seven muscle spindle and tendon organ afferents were compiled from stored data. The relationships between the firing profiles and the displacement and force signals were analysed with the help of mathematical models of the response characteristics of spindle primary and secondary afferents and tendon organs.

3. Whereas the firing of hamstring spindle afferents could be predicted with reasonable accuracy from the length and velocity signals alone, the firing profiles of triceps surae spindle afferents deviated from the predicted profiles, particularly during electromyogram (EMG) activity. This indicated that the components of fusimotor action linked to extrafusal muscle activity were significant in triceps surae, possibly because this muscle is more strongly recruited in the cat step cycle.

4. From the limited data available, it was not possible to identify the 'best' or most general mathematical function to predict spindle secondary firing. In the two triceps surae spindle secondary units studied, firing was well predicted by using the simplest possible model, rate proportional to displacement, whereas in the hamstring spindle secondary data, a more complex linear transfer function was needed. The results of modelling the spindle secondary data were consistent with a modest amount of phasic, static fusimotor action linked to EMG activity.

5. The averaged ensemble of tendon organ afferent activity from the triceps surae gave predictions of whole-muscle force that agreed well with separate triceps force measurements in normal cat locomotion. This supports the idea that ensembles of tendon organ afferents signal whole-muscle force.

6. Our overall conclusion is that to a first approximation, large muscle afferents in the cat hindlimb signal muscle velocity, muscle length and muscle force, at least in movements of the speed and amplitude seen in locomotion.

Many recordings have been obtained from muscle afferents in awake humans, monkeys, cats and rabbits, but nearly all the published data are in the form of firing profiles of individual afferents recorded during short sequences of movement. Because spindle afferents exhibit a broad range of response behaviours, it has been difficult to form an overall picture of the signals conveyed by *ensembles* of these receptors during normal movement. The obstacle to compiling population data has been to obtain enough recordings from afferents of a given type (spindle primary, spindle secondary or tendon organ) from a given muscle, in a reproducible motor task. The most comprehensive human neurography data in this regard are probably those of Al-Falahe, Nagaoka & Vallbo (1990), who documented the firing of seventeen spindle and eight tendon organ afferents during slow imposed and active sinusoidal movements performed against small loads. Although no attempt was made to compute averaged ensemble firing profiles, the firing characteristics of the individual afferents led to the qualitative conclusion that 'tendon organs behave as monitors of the amount of muscle contraction whereas spindles behave as stretch receptors'.

A start was made a few years ago on a 'look-up chart' of ensemble afferent firing profiles during locomotion in muscles of the cat hindlimb (Prochazka, Trend, Hulliger & Vincent, 1989*b*). From the limited data available it was concluded that the modulation of ensemble firing rate of spindle afferents was largely attributable to the length variations of the spindle-bearing muscles. A smaller part of the modulation appeared to result from transient changes in muscle fibre length due to tendon strain and muscle unloading in specific parts of the step cycle. Surprisingly

little modulation was attributable to phasic γ-fusimotor action linked to α-motoneuronal activation (α–γ linkage). In fact it was concluded that fusimotor action was set to different, fairly steady levels according to motor task and that phasic components of spindle primary firing due to α–γ linkage only became pronounced in rapid, forceful muscle contractions. These inferences were rather qualitative and based on small sets of data. Although some mathematical modelling of ensemble firing profiles has been performed for the purpose of estimating changes in spindle afferent stretch sensitivity (Prochazka & Hulliger, 1983; Gorassini, Prochazka & Taylor, 1993), so far this approach has never been applied to estimating the strength of *α-linked* components of fusimotor action in ensemble spindle afferent data. In this and the previous paper (Prochazka & Gorassini, 1998), we have derived such estimates from the discrepancies between the recorded firing rate profile and those estimated from muscle length signals with mathematical models.

A larger data base of chronic recordings from muscle afferents recorded during locomotion has now been collected. It is therefore of interest to up-date the previous ensemble firing profiles. Analysis of the new data with the use of mathematical models allows more reliable inferences regarding the underlying fusimotor action and provides a framework for predicting spindle afferent firing in many different muscles.

METHODS

The chronic data in this report were obtained from archives of previous studies in this laboratory. The recordings were obtained from thirty-four freely moving adult cats. All of the surgical and recording techniques used have been described in detail elsewhere and were summarized in the previous paper (Prochazka & Gorassini, 1998). Ensemble firing profiles of spindle primary and secondary and tendon organ afferents are presented.

Mathematical modelling

The averaged profiles were analysed on the basis of three mathematical models. The first was the spindle primary model that provided the best overall performance in the previous paper:

$$f = 4{\cdot}3\ v^{0{\cdot}6} + d + f_{\mathrm{m}},$$

where f is the firing rate (s^{-1}), v is muscle velocity ($\mathrm{mm\ s}^{-1}$), d is muscle displacement (mm) and f_{m} is the mean firing rate (s^{-1}).

Components of response mimicking α–γ linkage were added in some cases. These components were derived from the measured EMG signals, on the assumption that the EMG reflected the time course of α and γ activation. The second model was that of Poppele & Bowman (1970), describing spindle secondary afferents. Finally, we used the Houk & Simon (1967) transfer function describing tendon organ afferents. As in the previous paper (Prochazka & Gorassini, 1998), the ensembles were built up from the raw data using DASA2, a custom data analysis program. Matlab 4.2c and Simulink 1.3c software (Mathworks Inc., Natick, MA, USA) were used to implement the models in graphical form (see Appendix of previous paper). The graphical representation of the models and the Simulink simulation routines provide a convenient means of using the models, which may be downloaded from the following Internet website: http://gpu.srv.ualberta.ca/~aprochaz/hpage.html. Sigmaplot 3.1 ond 4.0 software (SPSS Inc., Chicago, IL, USA) was used for statistical regression analysis of the modelled responses.

RESULTS

The firing profiles of forty-seven muscle afferents recorded in thirty-four awake cats during overground locomotion are analysed in this report. Figure 1*A* shows a segment of a recording from a triceps surae spindle secondary afferent recorded over four step cycles along with muscle length and EMG activity. The afferent activity is presented as an instantaneous firing rate where the ordinate of each point is the inverse of the last firing interval. The dotted vertical lines mark alignment times selected with the averaging program. We aligned cycles to peak muscle length, which in this case occurred towards the end of the swing phase of the step cycle, some 70 ms prior to the foot making contact with the ground. Figure 1*B* shows the averaged profiles of EMG, length and afferent firing rate of the data in Fig. 1*A*. As in the previous paper (Prochazka & Gorassini, 1997), the firing rate is shown as a probability density function obtained by summing the action potentials occurring within consecutive bins and dividing by the bin width (in this case 0·01 s) to obtain mean rate per bin. Notice that the resolution of the probability density function is poor for this small number of steps. Because in some cases we only had data from two or three afferents of a particular type in a given muscle, the number of cycles contributed by each afferent was increased to improve the resolution of the rate function (sixteen cycles for single-afferent profiles, eight cycles for two-afferent profiles and four or five cycles for ensembles of three afferents or more).

Figure 2 shows averaged profiles of muscle length and afferent firing rate for eleven triceps surae spindle primary afferents. The firing rate profile is repeated four times in the figure, in each case overlaid with the predictions of a model. The data were derived from step cycles aligned to peak muscle length as described above. Each afferent contributed four step cycles. The issue here was the same as that in Fig. 2 of the previous paper (Prochazka & Gorassini, 1998), namely whether the relatively simple predictions of spindle primary firing from velocity and displacement alone could be enhanced by adding EMG-linked components of spindle firing. Figure 2*A* shows the prediction of the best model from the previous paper ($f = 4{\cdot}3v^{0{\cdot}6} + 2d +$ mean rate). The prediction was clearly in error in the middle portion of the profile. As in the previous paper, three signals representing EMG-linked fusimotor action were derived from the normalized rectified and averaged EMG. The first signal was obtained by scaling up the EMG by a factor of 50 (Fig. 2*Ba*). The second was a differential component computed with the function: $f = \mathrm{EMG}120(s+1)/(s+20)$, where f is the predicted rate (s^{-1}) and s is the Laplace operator (Fig. 2*Ca*). The third was an integrated component obtained with the function $f = \mathrm{EMG}500/(s+8)$ (Fig. 2*Da*). The integrated signal was time-advanced by 75 ms to mimic the fusimotor profiles in the literature, which slightly precede and outlast

the EMG bursts (Taylor & Donga, 1989). Adding the simple scaled EMG signal (Fig. 2*Ba*) to the prediction of the basic model in Fig. 2*A* slightly detracted from the fit (Fig. 2*Bb*: $r^2 = 0{\cdot}43$, r.m.s. error = 29·2, i.e. 29·2% of modulation depth of the target profile, which was 100 s^{-1}). However, an improvement was obtained with the addition of the differentiated EMG signal shown in Fig. 2*Ca* (Fig. 2*Cb*: $r^2 = 0{\cdot}62$, r.m.s. error = 24·5 s^{-1}, i.e. 24·5% of target modulation depth). The integrated EMG (Fig. 2*Da*) did not improve the fit (Fig. 2*Db*).

Overall, the only reasonable fit was that in Fig. 2*Cb* but even this was not as good as the fits obtained for the hamstring spindle primary data in the previous paper. Errors were particularly large around foot lift and foot contact. Several factors might have contributed to the errors. First, sonography studies have indicated that at the end of the stance phase of gait, where the triceps surae muscle switches from shortening to lengthening, there can be a short period of complete muscle unloading (Hoffer, Caputi, Pose & Griffiths, 1989). During the unloading, muscle spindles would not follow the length changes measured between origin and insertion of the parent muscle by our transducer, i.e. they would not show the same drop in firing rate as expected from the length signal alone. At the onset of the swing phase, the overlying knee flexor muscles have a burst of activity, which could cause local compression of triceps and thus some extra spindle firing. Another factor is tendon strain. Triceps muscle force rapidly increases at the onset of the stance phase which stretches the triceps tendon

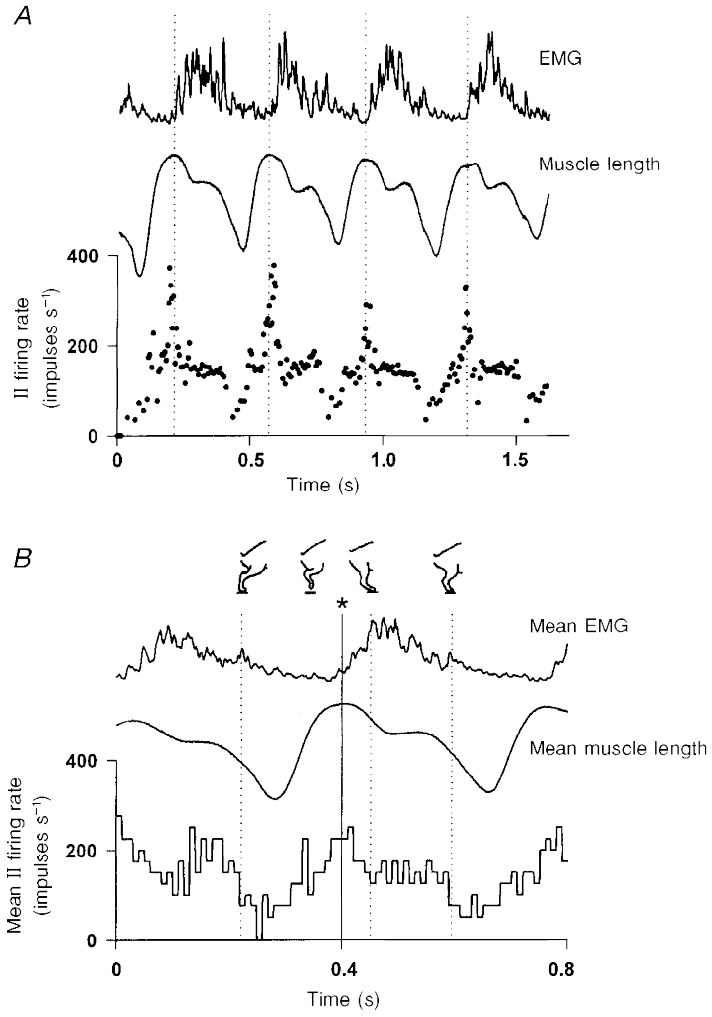

Figure 1. Illustration of averaging technique

A, instantaneous firing rate of a triceps surae spindle secondary afferent during four step cycles (bottom trace). The corresponding rectified and smoothed EMG of the receptor bearing muscle is shown in the top trace along with the origin to insertion length changes (middle trace) during stepping. Dotted lines show alignment points for averaging. *B*, mean EMG, muscle length and afferent firing rate of the four cycles in *A*. The mean rate was computed as a probability density function of impulses occurring in 10 ms bins. Schematics of hindlimb at top (and associated dotted vertical lines) show approximate timing of the different phases of the averaged step cycle. Alignment point for average is indicated by the continuous vertical line. The afferent fired most during muscle lengthening in the swing phase.

slightly so that spindles 'see' slightly less of the origin-to-insertion length (Hoffer *et al.* 1989; Elek, Prochazka, Hulliger & Vincent, 1990; Griffiths, 1991). At the end of the stance phase, the tendon is unloaded and therefore shortens slightly, *adding* a small component of length to the spindles that is not registered by the length transducer. Both of these factors would reduce the shortening of the spindle at the stance–swing transition, and cause a phase advance of spindle firing, as seen in the target profile in Fig. 2. At the onset of stance on the other hand, tendon strain would cause the opposite error in our length signal, i.e. the spindles would actually be shortening more than the recorded length signal. This has a bearing on our estimate of α–γ linkage, because the shortening seen by the spindles would lead us to underestimate how much additional phasic fusimotor action would be required to offset this shortening. Finally, the skin slips 10 mm or more over the femoral origin of triceps surae, mainly in the late stance phase when the knee extends. The proximal fixation thread of the length gauge emerges through the skin just distal to this point. During the implantation procedure, the point of emergence is carefully aligned with the origin and insertion of the muscle. However, in some cats, this alignment may not have been optimal and the skin may have tugged the length gauge slightly out of alignment, generating errors which would be most marked at the stance–swing and swing–stance transitions. Because the afferents and models of them are sensitive to velocity, even small measurement errors of this type could lead to significant errors in the predictions. This is a basic limitation of our chronic recording technique.

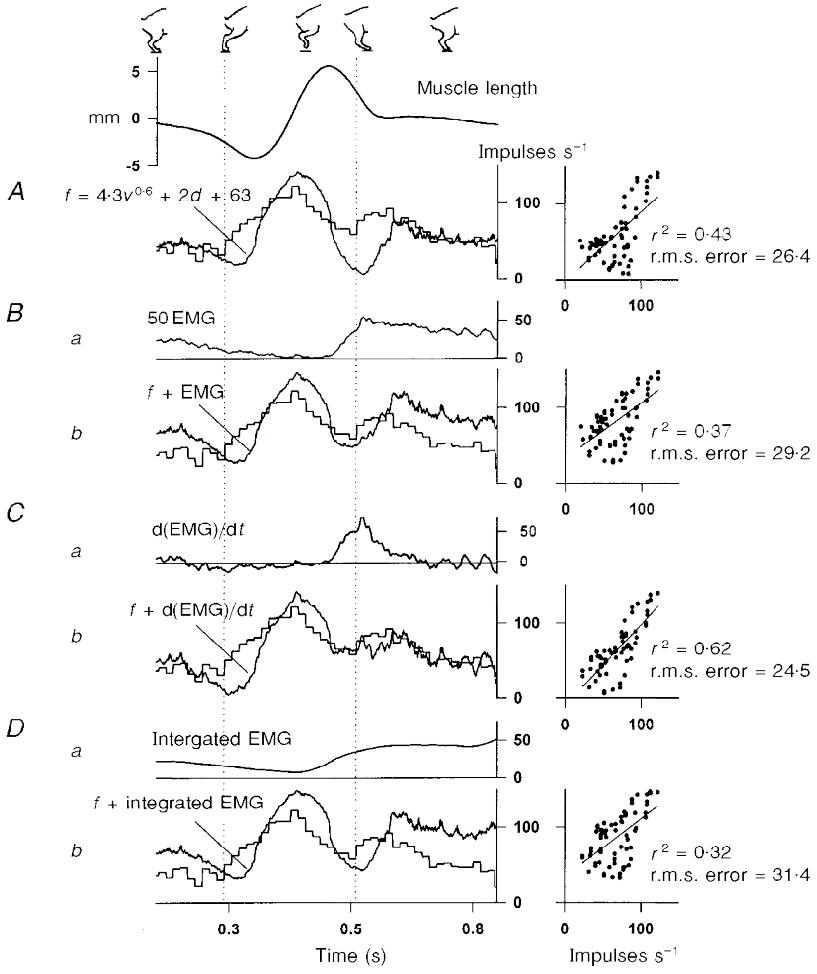

Figure 2. Predictions of triceps spindle primary afferent firing with added EMG-linked components mimicking α–γ linkage

The model used was the best overall model as determined in the previous study on hamstring spindle primary afferents. The offset (63 s^{-1}) was the mean firing rate over the cycles analysed. The fit in *A* shows significant errors, particularly just after foot lift-off and around foot touch-down. The addition of EMG-linked components (*Ba–Da*) tended to improve the fits (*Bb–Db*), particularly in *Ca*. To the right of each graph, the linear regression of the predicted rate (ordinate) is plotted against the 'real' rate (abscissa), one sample per bin. Note that the amplitude of the EMG components was relatively large (50 s^{-1} peak). A range of amplitudes was explored in repeated iterations. The data in *Ca* and *Cb* represent the best fit obtained in all the iterations. Possible reasons for the discrepancy at foot lift-off are discussed in the text.

Very few recordings from spindle secondary afferents have been obtained in voluntary movement in any species, because the axons are small in diameter and produce small extracellular action potentials. Figures 3 and 4 show data from two spindle secondary afferents. The speed of gait was markedly different in the two sets of data, so we analysed the units separately. Figure 3*A* shows the firing profile of unit 1 overlaid with a prediction obtained with the Poppele & Bowman (1970) spindle secondary transfer function:

$$f = 0{\cdot}59d(s + 0{\cdot}4)(s + 11)/(s + 0{\cdot}8) + 110,$$

where f is the firing rate (s^{-1}), 110 s^{-1} is the mean rate in the target profile, 0·59 is a scale factor chosen to give the optimal fit, d is muscle displacement (mm) and s is the Laplace operator. The very high mean firing rate of this afferent (110 s^{-1}) is indicative of strong static fusimotor drive (Jami & Petit, 1978).

The Poppele & Bowman model gave a mediocre prediction of the target profile (Fig. 3*A*: $r^2 = 0{\cdot}35$, r.m.s. error = 29·9, equivalent to 24% of the target modulation depth of 125 s^{-1}). In contrast to the spindle primary data, the prediction appeared to be phase-advanced over the target profile, so we tried a simpler transfer function with a higher-frequency turning point (i.e. less velocity sensitivity than the Poppele & Bowman model). This improved the fit (Fig. 3*B*: $r^2 = 0{\cdot}69$, r.m.s. error = 16·7% of modulation depth). An even better fit was obtained when the dynamic component was removed altogether (Fig. 3*C*: $r^2 = 0{\cdot}73$, r.m.s. error = 15·4% of modulation depth). Finally, as in previous figures, we mimicked α–γ linkage by adding to the

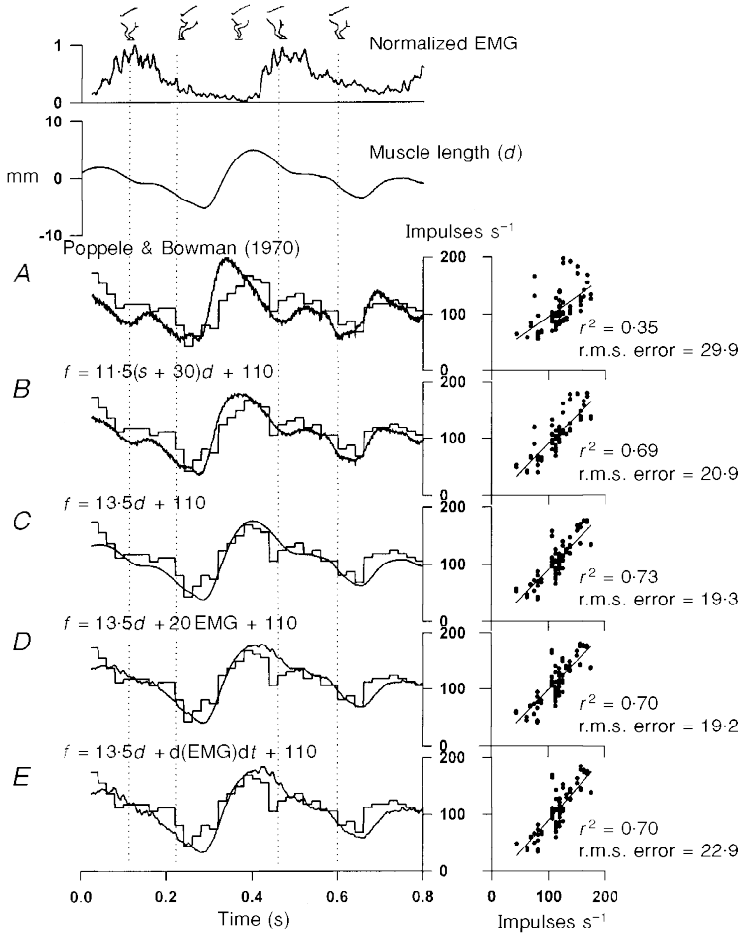

Figure 3. Predictions of the firing of a single triceps spindle secondary afferent with added EMG-linked components mimicking α–γ linkage

The data represent eight step cycles. Three models were used, the Poppele & Bowman (1970) group II model, and two *ad hoc* models of our own. The offset in each case (110 s^{-1}) was the mean firing rate of the afferent in the step cycles analysed. *A*, the prediction of the Poppele & Bowman model evidently showed too much phase advance. *B*, this prompted us to try a first order transfer function with less velocity sensitivity. Even this gave phase distortion. *C*, a simple proportional model gave the best overall fit. *D* and *E*, the addition to the predicted signal in *C* of proportional (*D*) and differential (*E*) EMG components with peak amplitudes of 30 s^{-1} neither improved nor detracted from the fits for this unit. In this figure and in Fig. 4, the bin widths for the mean frequency histograms were set to 20 ms.

prediction of the simple displacement model a signal proportional to the normalized rectified EMG shown at the top of Fig. 3. The best fit was obtained when the EMG scale factor was 20 (Fig. 3*D*: $r^2 = 0{\cdot}70$, r.m.s. error = 15·4% of modulation depth). Figure 3*E* shows the fit obtained when a differentiated version of the EMG was added, using the transfer function $f = \mathrm{EMG}40(s + 0{\cdot}5)/(s + 20)$. There was no statistically significant difference between the fits of Fig. 3*C*, *D* and *E* (Mann–Whitney rank sum test), i.e. the addition of EMG-linked components that added up to 30 s^{-1} to the firing rate neither improved nor detracted from the fits for this unit.

A similar analysis for the other triceps surae spindle secondary (unit 2) is shown in Fig. 4. Again the best fits were obtained using the simplest possible model, rate proportional to displacement (Fig. 4*C*: $r^2 = 0{\cdot}42$, r.m.s. error = 31·3% of modulation depth (125 s^{-1})). The addition of the normalized EMG signal, scaled up by 50 to mimic α–γ linkage, improved the fit substantially (Fig. 4*C*: $r^2 = 0{\cdot}64$, r.m.s. error = 16·2% of modulation depth). Finally, the addition of a dynamic version of the EMG signal obtained by using the filter transfer function $60(s + 0{\cdot}5)/(s + 20)$ produced a smaller improvement in fit over the simple prediction (Fig. 4*E*: $r^2 = 0{\cdot}46$, r.m.s. error = 25·1% of modulation depth). The mean firing rate of this unit (51 s^{-1}) indicated a low level of tonic fusimotor action.

Taking the data of Figs 2, 3 and 4 together, the evidence points to tonic, static fusimotor action with additional α-linked components of fusimotion that add up to 50 s^{-1} to the firing rate profile at peak EMG activity.

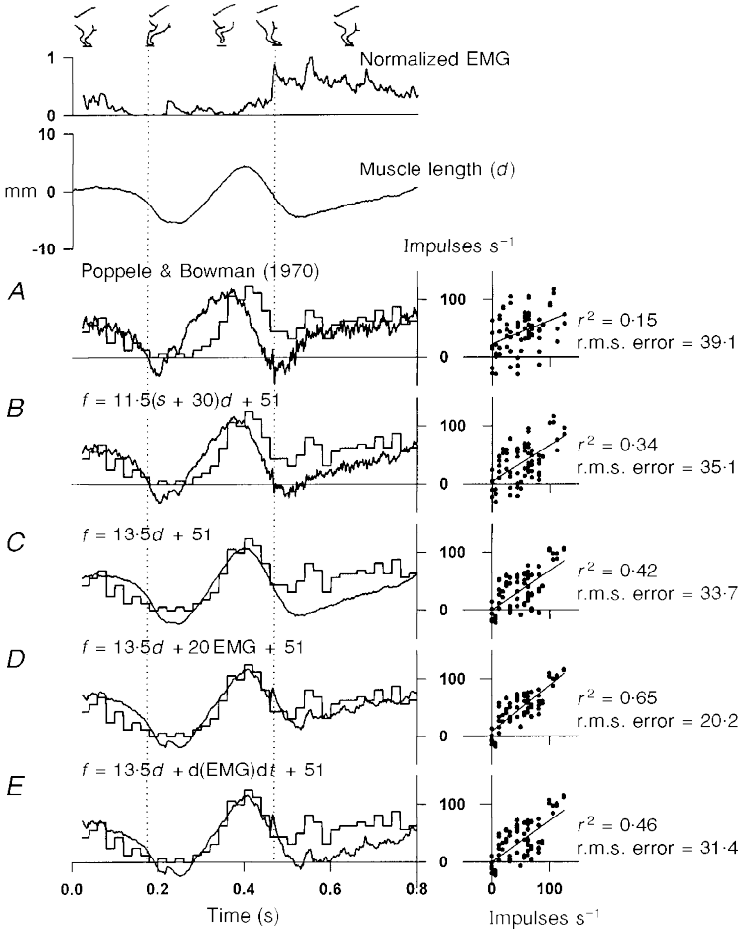

Figure 4. Predictions of the firing of a second triceps spindle secondary afferent with added EMG-linked components mimicking α–γ linkage

The data represent fourteen step cycles. The same models were used as in Fig. 3, with the offset adjusted to the mean firing rate of this unit (51 s^{-1}). *A*, the prediction of the Poppele & Bowman model again showed too much phase advance. *B*, the first order transfer function was an improvement, but still gave phase distortion. *C*, a simple proportional model gave a good overall fit, albeit with an underestimate of Ia rate during the stance phase. *D* and *E*, the addition to the predicted signal in *C* of proportional (*D*) and differential (*E*) EMG components with peak amplitudes of 20 s^{-1} significantly improved linearity and errors. Taken together, the data in *C*, *D* and *E* are consistent with a small EMG-linked component of firing rate in this group II afferent, suggesting a linkage of static fusimotor action with EMG.

By way of comparison, Fig. 5 shows data from a hamstring spindle secondary afferent. The mean firing rate was high (104 s^{-1}), consistent with strong tonic static fusimotor action. A satisfactory fit was obtained in this case with the Poppele & Bowman spindle secondary model (Fig. 54: $r^2 = 0{\cdot}8$, r.m.s. error 10·9% of modulation depth (190 s^{-1})). The addition of EMG-linked signals similar to those described above, but with peak amplitudes of 15 s^{-1}, did not significantly improve the fits. No EMG scale factors were found that actually improved the fit of the basic Poppele & Bowman model in this case, i.e. there was no clear evidence of EMG-linked fusimotor components but neither could one rule out small components of this type. This conclusion is much the same as that for hamstring spindle primary afferents.

Figure 6 shows a compilation of our data of ensemble muscle afferent firing in the cat step cycle. In cases where the length of the receptor-bearing muscle was not recorded, we aligned the cycles to peaks in either the hamstring or triceps surae length signals. The vertical lines are our estimates of the transitions between the swing and stance phases of the step cycle As far as we know this figure represents all of the available data of its type. Figure 6 may be viewed as an update of a previously published 'look-up chart' of hindlimb muscle afferent activity in the cat step cycle (Prochazka *et al.* 1989*b*). An interesting point to note is that all of the spindle primary profiles have fairly high mean firing rates (range, 50–110 s^{-1}). This indicates that offsets in Ia models should be around 75–80 s^{-1} to be representative of 'average' Ia responses. The high mean rates in both the spindle primary and secondary profiles argues strongly for a significant generalized background level of static fusimotor drive to all muscles of the hindlimb. Another interesting feature of Fig. 6 is the inclusion of length profiles predicted from afferent firing profiles by inverse models (see Fig. 5 in Prochazka & Gorassini, 1998). For spindle primary afferents we used the inverse of the hybrid power-law model used in Fig. 2. For spindle secondary afferents the inverse of the

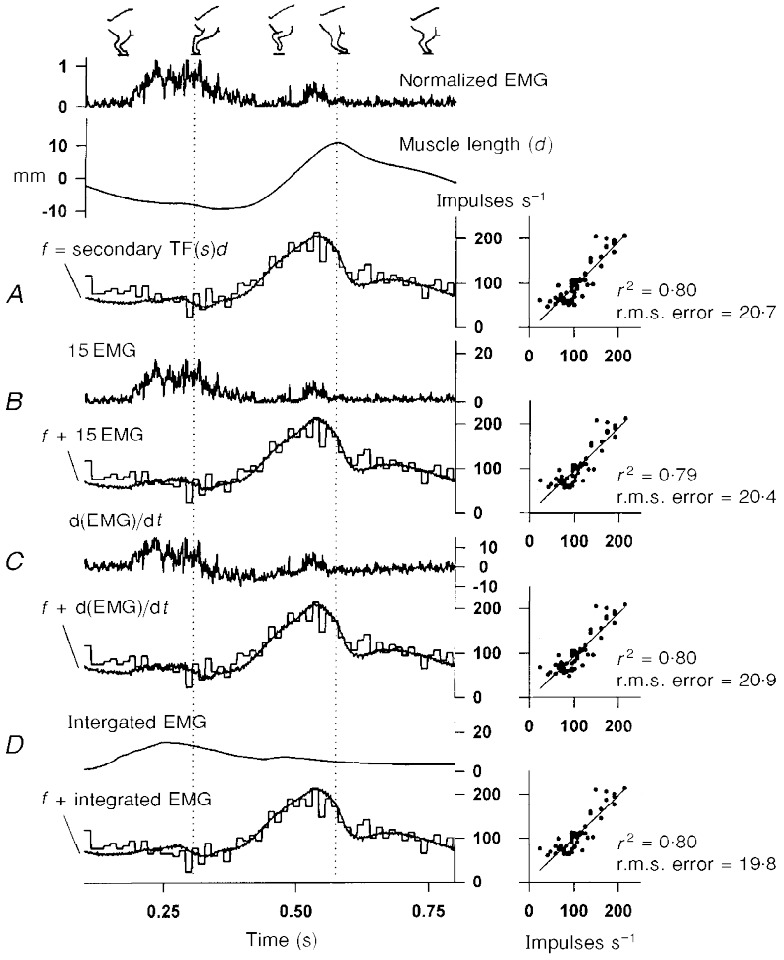

Figure 5. α–γ linkage test for hamstring spindle secondary afferent using analysis methods similar to those used in Figs 3 and 4

A, in this case, the Poppele & Bowman transfer function gave a very good fit. *B–D*, the addition of small EMG-linked components of firing rate did not substantially improve the fit, but neither was the fit worsened. The data show that a small component of firing linked to EMG activity, as implied in the data of Fig. 4, cannot be ruled out.

Poppele & Bowman secondary model was used. The length variations of plantaris, flexor and extensor digitorum longus and peroneus longus have never been measured, so the predicted length profiles in Fig. 6 are estimates that will await future verification. As a note of caution, one would expect the predictions to be inaccurate if phasic fusimotor activity and/or other factors such as changes in pennation angle and tendon compliance had caused significant modulation of the spindle firing rate. For the sake of completeness we have included our own representation of the data on muscle afferent firing in the vasti and sartorius published by Loeb & Duysens (1979), Loeb & Hoffer (1985), Loeb, Hoffer & Marks (1985*a*) and Loeb, Hoffer & Pratt (1985*b*).

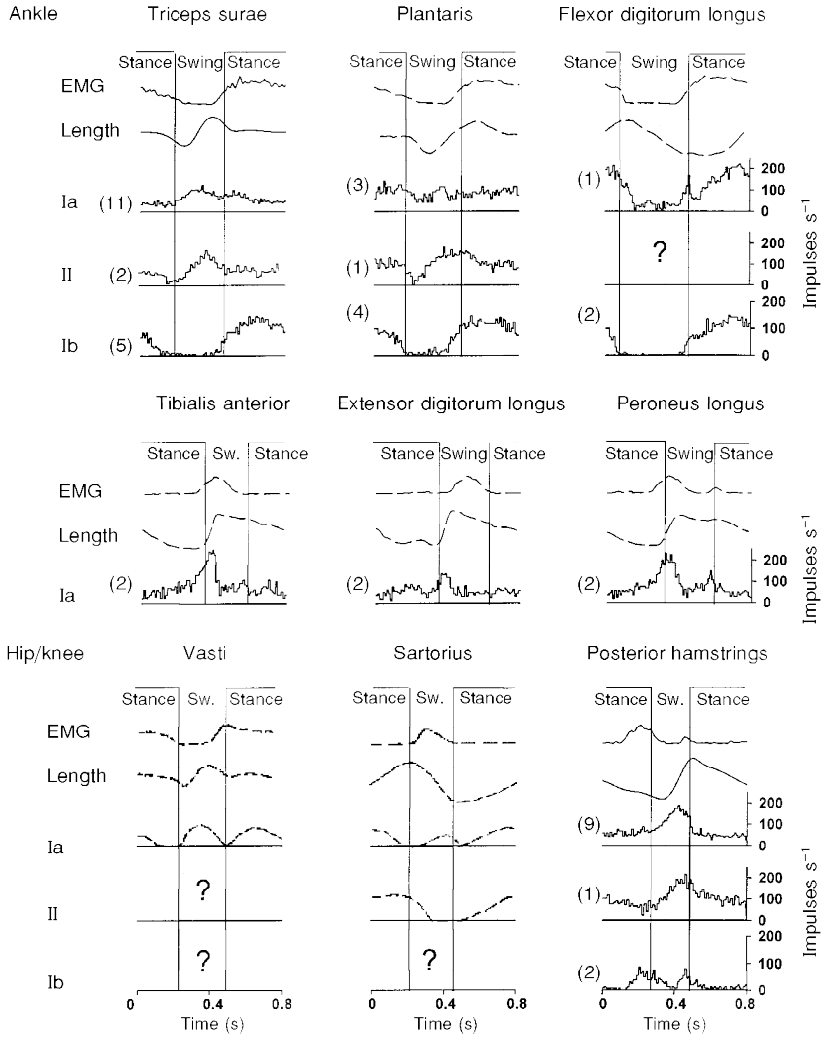

Figure 6. Up-dated look-up chart of ensemble afferent firing in the cat hindlimb

New afferent profiles added to the look-up chart include: flexor digitorum longus spindle primary and tendon organ, tibialis anterior spindle primary, extensor digitorum longus spindle primary, peroneus longus spindle primary and posterior hamstring spindle secondary. The up-dated number of afferents contributing to each average is shown to the left of the graph in parentheses. Step cycles were aligned to peaks in either the hamstring or triceps surae length signals (only shown for the triceps and hamstring data). In one case (triceps surae secondaries), the step cycle durations happened to be quite short, so these profiles were normalized along the time axis to match all the other plots. The length signals were also used to estimate stance–swing and swing–stance transitions in the step cycle (see vertical lines). When unavailable, representative EMG profiles (dashed lines) were taken from Rossignol (1996) and Rasmussen, Chan & Goslow (1978). Estimates of length (dashed lines) were obtained by using the inverse of the hybrid power law model for flexor and extensor digitorum longus, tibialis anterior and peroneus longus spindle primary afferents and the inverse of the Poppele & Bowman model for the plantaris secondary afferent. Note the high mean firing rates of spindle primary and secondary afferents, indicating a high background of static fusimotor drive to muscles of the hindlimb during stepping. The vasti and sartorius graphs are representations of data published by Loeb *et al.* (1985 *a*,*b*).

Figure 7 shows the ensemble firing rate data of four triceps surae tendon organ afferents. The profile reaches a peak rate of about 130 s^{-1}, and closely parallels the rectified EMG signal. We used the inverse of the Houk & Simon (1967) transfer function to obtain an estimate of the force signal 'seen' by the tendon organ afferents. This is compared with data obtained during the cat step cycle from buckle force transducers implanted on the soleus tendon of two cats (Herzog, Leonard & Guimaraes, 1993). These data were kindly supplied to us in digital form by Dr Walter Herzog. The figure shows that the predicted force signal closely matches the directly measured muscle force. This supports the idea that ensembles of tendon organ afferents signal whole-muscle force, a notion that has been in dispute recently (Jami, 1992; Jami, Petit, Zytnicki & Horcholle-Bossavit, 1992).

DISCUSSION

A knowledge of the firing properties of muscle afferents during voluntary movement is important for an understanding of the role of proprioceptive signals in motor control and sensory experience. In this and the preceding paper (Prochazka & Gorassini, 1998), we have collated much of the accessible data on the firing of muscle afferents in cat locomotion. Several general features of muscle spindle firing emerged from the ensemble data.

First, the mean firing rates of all of the muscle afferents in the step cycle were high (in the range 50–110 s^{-1}). The ensemble profiles in Fig. 6 showed that neither spindle primary nor secondary endings were completely silenced at any point in the step cycle, despite rapid shortening of the receptor-bearing muscles. This is consistent with asignificant

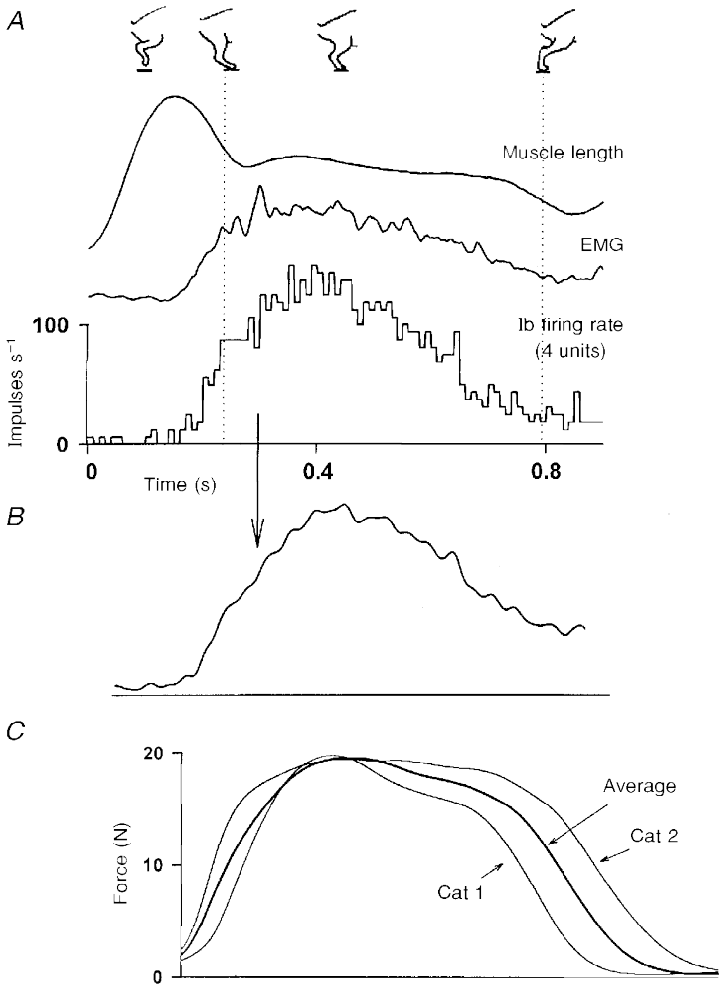

Figure 7. Ensemble data from four triceps surae tendon organ afferents

A, each afferent contributed four step cycles. Muscle force was not measured in our experiments. However, a prediction of force was obtained from the afferent rate profile with the use of the inverse of the tendon organ model of Houk & Simon (1967) in *B*. This was compared with force profiles obtained in separate experiments using an implanted buckle force transducer in *C*. The duration of the step cycles in *C* were normalized to match the time course of the predicted force in *B*. These data were kindly provided in digital form by Dr Walter Herzog (see Herzog *et al.* 1993). Note the good correspondence between the predicted and separately measured force profiles.

level of static fusimotor action in all the muscles sampled. The modulation depth about this high mean firing rate was generally also quite appreciable (100 s^{-1} or more), with peak rates of 150–200 s^{-1}. This is far in excess of the highest firing rates recorded in human neurography (e.g. Al-Falahe *et al.* 1990), which raises the question of whether a species difference is involved. Although our study does not resolve this issue, muscle velocity clearly emerged as a dominant variable in determining spindle primary firing rates. During locomotion in the cat, muscle velocities are more than an order of magnitude greater than the maximal muscle velocities in human neurography experiments (e.g. Al-Falahe *et al.* 1990). The results of the modelling in the previous paper (Prochazka & Gorassini, 1998) show that at low velocities, much lower spindle rates would be predicted and this is indeed what is observed in very slow, non-locomotor movements in cats. We would therefore argue that before a species difference is assumed, one should compare data collected under comparable motor circumstances.

Second, although the main variable in the step cycle determining the modulation of spindle primary afferent firing was muscle velocity, in triceps surae muscles, other modulatory influences were also at play. There was evidence, for example, of a significant α-linked component of fusimotor action in the triceps spindle primary data. Using the scaled EMG or its derivatives to provide biasing is admittedly a crude approach to modelling presumed α-linked γ action. However in the absence of a transfer function or other mathematical relationship to describe the coupling of γ to α action in normal movements, we felt that three simple models using proportional, integral and differential components of EMG were worth trying. The improvement in the goodness of fit in Figs 2 and 4 indicates that there was indeed value in this approach.

In addition, there was a component of spindle primary firing at the stance–swing transition that might have been due to tendon compliance effects or other mechanical transients, as discussed above. The triceps spindle primary firing profiles are therefore more complex and difficult than the hamstring spindle primary responses to model accurately. The important general point to emerge from our two studies was that since velocity is a key modulatory variable in spindle primary afferents and since the velocities in the step cycle are so high, it is a foregone conclusion that the firing rates of spindle primary afferents in the locomotor cycle are dominated by the time course of muscle velocity. In much slower movements, other modulatory influences such as α-linked fusimotor action would become more apparent. These conclusions are not really new, but the ensemble data underscores their validity.

In contrast to the spindle primary afferents, the firing rates of spindle secondary ensembles were more simply related to muscle length. The results of modelling the spindle secondary data in triceps surae and hamstring muscles were consistent with a modest amount of phasic, fusimotor action linked to EMG activity. Taken together with the spindle primary findings, we conclude that there is a component of static fusimotor action linked to the phasic contractions of the receptor-bearing muscle (i.e. α–γ_s linkage). This is in agreement with Gottlieb & Taylor (1983), Taylor & Donga (1989) and some of the conclusions of Bennett, De Serres & Stein (1996). We cannot rule out α-linked *dynamic* γ action (Murphy, Stein & Taylor, 1984; Greer & Stein, 1990; Murphy & Martin, 1993), because our technique of subtracting the predicted from actual afferent firing only identifies biasing. Some γ_d fibres do have a significant *biasing* action on spindle primary endings (Hulliger, 1984; Prochazka, 1996). Though the estimates are rather crude, the amount of α-linked γ action implied by the present analysis of the triceps surae spindle primary data certainly seems larger than previously proposed in publications from this laboratory (e.g. Prochazka, Hulliger, Zangger & Appenteng, 1985; Prochazka, 1996).

From the perspective of biomechanical modelling, the EMG-linked components of spindle secondary firing did not cause major errors in predictions of spindle secondary firing from the length signals alone. From the limited data available (three units), it was not possible to identify the 'best' or most general mathematical function to predict spindle secondary firing. For the triceps surae secondaries, scaling the length signal gave good fits, whereas the the hamstring secondary data were better fitted with the use of the Poppele & Bowman (1970) secondary transfer function. Unfortunately very few spindle secondary afferents have been recorded from during normal movement, so the precise nature of the best spindle secondary model remains open. A conservative approach would be to use a model that had slightly less velocity sensitivity than the Poppele & Bowman model.

The concept raised in the companion paper (Prochazka & Gorassini, 1998), of an offset or 'carrier' frequency, about which ensemble firing rates are modulated, deserves a little more discussion. As mentioned above, the mean firing rates in our spindle data ranged from 50 to 110 s^{-1}. Mean firing rates may be muscle specific, so the assumption of an 'average' representative offset of 75–80 s^{-1} may lead to errors for individual muscle afferent ensembles. It should also be understood that if a non-linear relationship is used to predict ensemble firing rate from velocity (e.g. $f = v^{0.6}$), and if the velocity profile is markedly asymmetrical, a net offset will be added to the offset in the model, i.e. to the mean rate of the predicted profile. In practice, we found that with the strongest non-linearity ($v^{0.3}$), the asymmetry of the length profile caused a deviation in mean firing rate of 17 s^{-1} (Fig. 3*C* in Prochazka & Gorassini, 1998).

The tendon organ data showed fairly clearly that the ensemble profiles of even a small number of units (four in Fig. 7) gave predictions of whole-muscle force that agreed well with separate triceps force measurements in normal cat locomotion. On the assumption that central second order cells involved in sensorimotor control receive convergent input from several afferents, our data would therefore

support the school of thought that the function of tendon organ afferents is to signal whole muscle force rather than internal forces related to individual motor units (Crago, Houk & Rymer, 1982; Jami, 1992; Jami *et al.* 1992). If in the future interneurons are found that respond to one or two tendon organ afferents only, this conclusion would need to be modified.

Considering the ensemble data as a whole, one is struck by the very high firing rates and depth of modulation of muscle afferent firing. Assuming that all of the muscle afferents in a limb fire at comparable mean frequencies (around 80 s^{-1}) and assuming about 10 000 of them in the hindlimb (Voss, 1971) the mean net input to the spinal cord during locomotion would be 800 000 action potentials s^{-1} (higher than estimated previously: Prochazka, Hulliger, Trend, Llewellyn & Dürmüller, 1989*a*). In motor tasks such as stepping, the bulk of the information being signalled appears to relate to the mechanical events taking place, rather than to phasic fusimotor signals. In other words, theories of fusimotor control that espouse follow-up servo control, efference copy or a predictive neutralization of the sensory response to expected mechanical variations (e.g. Phillips, 1969) are not supported by our data. Our overall conclusion is that to a first approximation, the large muscle afferents signal muscle velocity, muscle length and muscle force, at least in movements of the speed and amplitude seen in locomotion.

Al-Falahe, N. A., Nagaoka, M. & Vallbo, A. B. (1990). Response profiles of human muscle afferents during active finger movements. *Brain* **113**, 325–346.

Bennett, D. J., De Serres, S. J. & Stein, R. B. (1996). Regulation of soleus muscle spindle sensitivity in decerebrate and spinal cats during postural and locomotor activities. *Journal of Physiology* **495**, 835–850.

Crago, P. E., Houk, J. C. & Rymer, W. Z. (1982). Sampling of total muscle force by tendon organs. *Journal of Neurophysiology* **47**, 1069–1083.

Elek, J., Prochazka, A., Hulliger, M. & Vincent, J. (1990). In-series compliance of gastrocnemius muscle in cat step cycle: do spindles signal origin-to-insertion length? *Journal of Physiology* **429**, 237–258.

Gorassini, M., Prochazka, A. & Taylor, J. (1993). Cerebellar ataxia and muscle spindle sensitivity. *Journal of Neurophysiology* **70**, 1853–1862.

Gottlieb, S. & Taylor, A. (1983). Interpretation of fusimotor activity in cat masseter nerve during reflex jaw movements. *Journal of Physiology* **345**, 423–438.

Greer, J. J. & Stein, R. B. (1990). Fusimotor control of muscle spindle sensitivity during respiration in the cat. *Journal of Physiology* **422**, 245–264.

Griffiths, R. I. (1991). Shortening of muscle fibres during stretch of the active cat medial gastrocnemius muscle: the role of tendon compliance. *Journal of Physiology* **436**, 219–236.

Herzog, W., Leonard, T. R. & Guimaraes, A. C. (1993). Forces in gastrocnemius, soleus, and plantaris tendons of the freely moving cat. *Journal of Biomechanics* **26**, 945–953.

Hoffer, J. A., Caputi, A. A., Pose, I. E. & Griffiths, R. I. (1989). Roles of muscle activity and load on the relationship between muscle spindle length and whole muscle length in the freely walking cat. In *Afferent Control of Posture and Locomotion*, ed. Allum, J. H. J. & Hulliger, M., *Progress in Brain Research*, vol. 80, pp. 75–86. Elsevier, Amsterdam.

Houk, J. C. & Simon, W. (1967). Responses of Golgi tendon organs to forces applied to muscle tendon. *Journal of Neurophysiology* **30**, 1466–1481.

Hulliger, M. (1984). The mammalian muscle spindle and its central control. *Reviews of Physiology, Biochemistry and Pharmacology* **101**, 1–110.

Jami, L. (1992). Golgi tendon organs in mammalian skeletal muscle: Functional properties and central actions. *Physiological Reviews* **72**, 623–666.

Jami, L. & Petit, J. (1978). Fusimotor actions on sensitivity of spindle secondary endings to slow muscle stretch in cat peroneus tertius. *Journal of Neurophysiology* **41**, 860–869.

Jami, L., Petit, J., Zytnicki, D. & Horcholle-Bossavit, G. (1992). Unloading: a reason why individual golgi tendon organs cannot measure muscle force, In *Muscle Afferents And Spinal Control of Movement*, ed. Jami, L., Pierrot-Deseilligny, E. & Zytnicki, D., pp. 71–76. Pergamon Press, London.

Loeb, G. E. & Duysens, J. (1979). Activity patterns in individual hindlimb primary and secondary muscle spindle afferents during normal movements in unrestrained cats. *Journal of Neurophysiology* **42**, 420–440.

Loeb, G. E. & Hoffer, J. A. (1985). Activity of spindle afferents from cat anterior thigh muscles. II. Effects of fusimotor blockade. *Journal of Neurophysiology* **54**, 565–577.

Loeb, G. E., Hoffer, J. A. & Marks, W. B. (1985*a*). Activity of spindle afferents from cat anterior thigh muscles. III. Effects of external stimuli. *Journal of Neurophysiology* **54**, 578–591.

Loeb, G. E., Hoffer, J. A. & Pratt, C. A. (1985*b*). Activity of spindle afferents from cat anterior thigh muscles. I. Identification and patterns during normal locomotion. *Journal of Neurophysiology* **54**, 549–564.

Murphy, P. R. & Martin, H. A. (1993). Fusimotor discharge patterns during rhythmic movements. *Trends in Neurosciences* **16**, 273–278.

Murphy, P. R. Stein, R. B. & Taylor, J. (1984). Phasic and tonic modulation of impulse rates in γ motoneurons during locomotion in premammillary cats. *Journal of Neurophysiology* **52**, 228–243.

Phillips, C. G. (1969). Motor apparatus of the baboon's hand. The Ferrier Lecture, 1968. *Proceedings of the Royal Society* B **173**, 141–174.

Poppele, R. E. & Bowman, R. J. (1970). Quantitative description of linear behaviour of mammalian muscle spindles. *Journal of Neurophysiology* **33**, 59–72.

Prochazka, A. (1996). Proprioceptive feedback and movement regulation. In *Handbook of Physiology*, section 12, *Exercise: Regulation and Integration of Multiple Systems*, ed. Rowell, L. & Sheperd, T., pp. 89–127. American Physiological Society, New York.

Prochazka, A. & Gorassini, M. (1998). Models of ensemble firing of muscle spindle afferents recorded during normal locomotion in cats. *Journal of Physiology* **507**, 277–291.

Prochazka, A. & Hulliger, M. (1983). Muscle afferent function and its significance for motor control mechanisms during voluntary movements in cat, monkey and man. In *Motor Control Mechanisms in Health and Disease*, ed. Desmedt, J. E., pp. 93–132. Raven Press, New York.

Prochazka, A., Hulliger, M., Trend, P. St J., Llewellyn, M. & Dürmüller, N. (1989*a*). Muscle afferent contribution to control of paw shakes in normal cats. *Journal of Neurophysiology* **61**, 550–562.

Prochazka, A., Hulliger, M., Zangger, P. & Appenteng, K. (1985). 'Fusimotor set': new evidence for α-independent control of γ-motoneurones during movement in the awake cat. *Brain Research* **339**, 136–140.

Prochazka, A., Trend, P., Hulliger, M. & Vincent, S. (1989*b*). Ensemble proprioceptive activity in the cat step cycle: towards a representative look-up chart. In *Afferent Control of Posture and Locomotion*, ed., Allum, J. H. J. & Hulliger, M, *Progress in Brain Research*, vol. 80, pp. 61–74. Elsevier, Amsterdam.

Prochazka, A. & Wand, P. (1981). Independence of fusimotor and skeletomotor systems during voluntary movement. In *Muscle Receptors and Movement*, ed. Taylor, A. & Prochazka, A., pp. 229–243. Macmillan Publishers Ltd, London.

Rasmussen, S., Chan, A. K. & Goslow, G. E. (1978). The cat step cycle: electromyographic patterns for hindlimb muscles during posture and unrestrained locomotion. *Journal of Morphology* **155**, 253–270.

Acknowledgements

This work was supported by the Canadian Medical Research Council and the Alberta Heritage Foundation for Medical Research.

Corresponding author

A. Prochazka: Division of Neuroscience, University of Alberta, Edmonton, Alberta, Canada T6G 2S2.

Email: arthur.prochazka@ualberta.ca